PHYSICAL REVIEW A **66**, 062505 (2002)

Ionization potentials of internal conversion electrons for the superheavy elements 112, 114, 116, and 118

Nicola Gaston and Peter Schwerdtfeger*
Department of Chemistry, University of Auckland, Private Bag 92019 Auckland, New Zealand

Witold Nazarewicz
Department of Physics and Astronomy, University of Tennessee, Knoxville, Tennessee 37996;
Physics Division, Oak Ridge National Laboratory, P.O. Box 2008, Oak Ridge, Tennessee 37831;
and Institute of Theoretical Physics, Warsaw University, Ulnicka Hoża 69, Warsaw PL-00681, Poland

(Received 5 September 2002; published 26 December 2002)

K-shell $(1s)$ and L-shell $(2s)$ ionization potentials for the superheavy elements with $Z=112$, 114, 116, and 118 are predicted to an accuracy of a few 10 eV using Dirac-Hartree-Fock theory and taking into account quantum electrodynamic and nuclear-size effects. The data obtained are for any number of electrons and can be used in the future in theoretical and experimental studies of these elements involving K-electron conversion spectroscopy.

DOI: 10.1103/PhysRevA.66.062505 PACS number(s): 32.10.Hq, 31.30.Jv, 31.15.Ar, 21.10.Ky

I. INTRODUCTION

The synthesis of new superheavy elements promises to contribute a great deal to our fundamental understanding of both nuclear physics and chemistry [1]. Yet before these atoms can be properly examined, they need to be reliably and unambiguously prepared and detected. The use of α-correlation spectroscopy as a detection technique is well understood and established for new transactinide elements, however, the daughter nuclides produced in α-decay chains of the longer-lived superheavy species are likely not to extend into a well-known region of the periodic table of isotopes [1,2]. This leads to the recognition that additional spectroscopic methods of analysis are required [3]. The synthesis of the superheavy elements up to $Z=112$ has been confirmed by now [4]. The syntheses of the elements with nuclear charge 114 and 116 have also been announced very recently [5,6]. However, in neither of these cases do the α chains end up at a known isotope so a firm assignment could not be made.

Various experimental methods for the identification of unknown superheavy elements have been proposed including mass separation and chemical studies [7]. In this work, we concentrate on atomic aspects. A good spectroscopic signature of an element is the characteristic electron and x-ray spectrum associated with internal conversion [8]. The deformed excited nucleus produced through fusion is likely to undergo a rotational transition on a very short time scale $(10^{-20}$ s), which can produce an inner-shell vacancy in the atom. Electron conversion usually dominates the lowest rotational transitions in heavy well-deformed (or superdeformed) nuclei, where transition energies are similar to energies of K- and L-shell ionization. Spectacular examples are conversion electron spectroscopy studies in the superdeformed minimum of ^{240}Pu [9] or rotational spectroscopy of the heavy elements such as $^{252-234}$No [10]. The emitted electron may be easily detected by electron spectrometers (currently to an accuracy of about 1 keV) [11], and its kinetic energy is indicative of the rotational transition in a nucleus. This could be used to identify a nucleus provided that some information existed on the actual energy of an excited state. Here, theoretical calculations and systematics of experimental data could come to the rescue. For instance, moments of inertia of rotational bands in well-deformed nuclei can be reasonably estimated using calculated equilibrium deformations [12]. (For recent calculations of rotational properties of the heaviest elements, see Ref. [13].) Unfortunately, the spectroscopic data on the heaviest and superheavy elements are still very scarce. In addition to the nobelium data of Ref. [10], there have been $\alpha-\gamma$ decay studies, in which a number of excited states in this region have been identified [14]. The good news is that many heavy and superheavy nuclei are expected to be deformed in their ground states (see Ref. [15], and references quoted therein). The pattern of predicted equilibrium deformations is fairly robust, i.e., it weakly depends on model details. Namely, for $N<176$, most of the heaviest nuclei are calculated to be prolate, and they are spherical for $N>180$. These two regions are separated by a narrow band of transitional nuclei with small equilibrium deformations. The largest deformations are obtained for nuclei around ^{254}No. The stabilizing role of deformation in the region of the known heaviest elements has been attributed to the deformed shell gaps at $N=162$ and $Z=108$ [15]. It is, therefore, anticipated that some nuclei belonging to α-decay chains of unknown superheavy elements with $Z>112$ are in fact deformed [16].

The process of internal conversion is coupled by the electromagnetic field, quantized in the form of a photon, and is, therefore, most important for the $1s$ and $2s$ electrons in heavy atoms [17]. In fact, the probability of this process is so high for the superheavy elements that it may well occur while the atom is still in a highly ionized state resulting from the acceleration process. The potential application of conver-

---

*Email address: p.schwerdtfeger@auckland.ac.nz

©2002 The American Physical Society

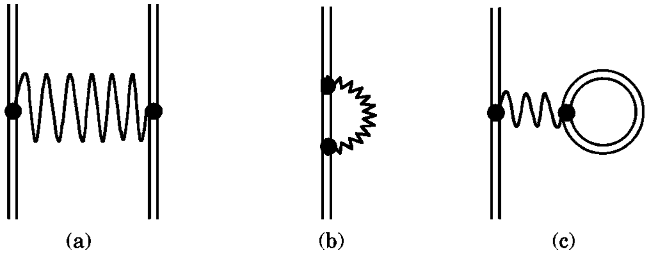

FIG. 1. Feynman representation. (a) The Breit interaction: photon exchange between electrons. (b) Electron self-energy: creation and annihilation of a virtual photon. (c) Vacuum polarization (photon self-energy): creation and annihilation of an electron-positron pair in the nuclear Coulomb field.

sion electron spectroscopy has motivated a quantity of theoretical work on superheavy elements; for instance, the calculations of internal-conversion coefficients [18,19]. We mention that K and L autoionization (electron shake off) are also well known for other nuclear decay processes such as α and β decay [20].

For the identification of superheavy elements, accurate ionization potentials (E_{ion}) are required, which can be derived from relativistic *ab initio* theory for the atoms in different states of ionization. Taking the energy difference between the neutral atom and the inner-shell ionized product allows valence electron relaxation to be included. It is now well accepted that for heavy atoms, relativistic effects are very important [21]. While Dirac-Fock calculations are fully relativistic (although quantization of the electromagnetic field is neglected) for the inner shells of superheavy atoms, additional quantum electrodynamic (QED) contributions can no longer be ignored. The Breit term is commonly included to account for magnetic and retarded photon exchange. However, smaller corrections due to radiative interactions such as the self-energy (SE) and vacuum polarization (VP) should also be considered (see Fig. 1). Here we present the results of such calculations. We mention that radiative contributions to valence (outer shell) energies in superheavy elements can even be as large as 0.5% of the total ionization potential [22].

This paper is laid out as follows. First, a brief overview of the technical aspects of the calculations is given in Sec. II, including a discussion of relativistic and QED effects. Section III discusses the expected accuracy of our calculations in light of the available experimental data. The K-shell $(1s)$ and L-shell $(2s)$ ionization potentials are given in Sec. IV for the superheavy elements 112, 114, 116, and 118 as a function of the number of electrons N_E ($N_E=1$–Z; Z is the nuclear charge of the atom). Finally, conclusions are contained in Sec. V.

II. DIRAC-FOCK CALCULATIONS

Dirac-Hartree-Fock (DHF) calculations [23] were performed using the Dirac-Coulomb operator for a multielectron system,

$$D=\sum_i \{c\vec{\alpha}_i\vec{p}_i+c^2\beta_i+V_{ext}(i)\}+\sum_{i<j}\frac{1}{r_{ij}}, \tag{1}$$

where $\vec{\alpha}$ and β are the well-known Dirac matrices in the standard representation. The external potential is the standard Coulombic potential accounting for the finite extension of the nucleus [finite nucleus model, (FNM)]. For the FNM, we chose a two-parameter Fermi-type charge distribution [24],

$$\rho(r)=\frac{\rho_0}{1+e^{(r-b)/a}}. \tag{2}$$

The parameters a and b are taken from Ref. [25]. Note that in using the expression given in Eq. (2), we have $\rho(0)\neq\rho_0$ (for a detailed discussion, see Ref. [24]). For superheavy elements, the $1s$-shell radius becomes very small ($\langle r\rangle_{1s}=466.9$ fm for $Z=118$) and the influence of the finite nuclear size cannot be neglected anymore. Furthermore, Reiher and Kind have shown that a nonvariational treatment of the Breit effect is sufficient if the FNM is used [26]. Consequently, the Breit interaction has been treated as a perturbation to the Coulomb Hamiltonian. In this work, we applied the Breit interaction in the Coulomb gauge [27],

$$g_{ij}=-\frac{\vec{\alpha}_i\vec{\alpha}_j}{r_{ij}}e^{i\omega_{ij}r_{ij}}+(\vec{\alpha}_i\cdot\vec{\nabla}_i)(\vec{\alpha}_j\cdot\vec{\nabla}_j)\frac{e^{i\omega_{ij}r_{ij}}-1}{\omega_{ij}^2 r_{ij}}, \tag{3}$$

where r_{ij} is the distance between electrons and ω_{ij} is the energy of the exchange photon. As shown by Gaunt [28], in the low-frequency limit, Eq. (3) may be split into a part describing the magnetic electron-electron interaction and the term representing the relativistic retardation of the Coulomb exchange photon. The magnetic part is the dominant component being proportional to $1/r^3$ in the classical limit, and thereby highly important for the strongly interacting inner electrons in superheavy elements. The frequency dependence ω_{ij} is also included for improved accuracy.

The electron SE is a major contribution to the total Lamb shift and is obtained from the hydrogenic values of Mohr [29] using screened nuclear charge values for each orbital. In the hydrogenic approximation, the electron SE shift can be parametrized as

$$\Delta E=\frac{Z^4\alpha^3}{n^3\pi}F_n(Z\alpha), \tag{4}$$

where $\alpha=1/c$ is the fine-structure constant and F_n is of the form,

$$F_n(Z\alpha)=A_{40}+A_{41}\ln(Z\alpha)^{-2}+A_{50}Z\alpha+\cdots, \tag{5}$$

with the parameters determined by Mohr and co-workers [30]. It is well known that at high Z, the expansion (5) converges slowly ($Z\alpha$ is not an ideal expansion parameter for high Z) [31] and an exact treatment within the bound-state Furry picture of QED is required [32]. However, such a treatment is currently not feasible for many-electron systems with high nuclear charge and so we need to evaluate the accuracy of using Eq. (5) for K- and L-shell ionization potentials.

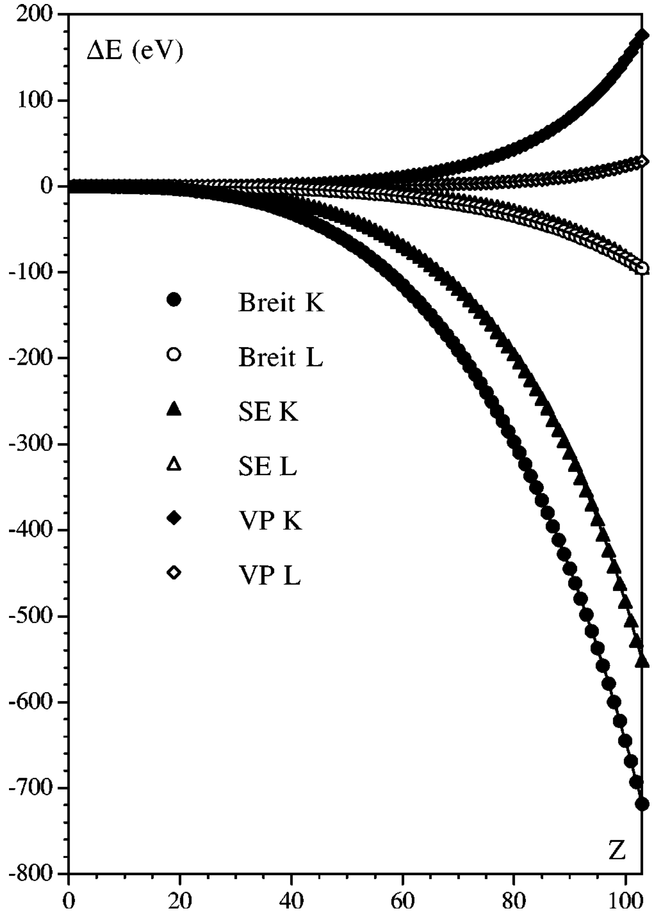

FIG. 2. Breit and other QED contributions (self-energy SE, vacuum polarization VP) to $K(1s)$- and $L(2s)$-shell ionization potentials for the neutral elements up to Lr ($Z=103$).

The VP term is evaluated according to the method of Fullerton and Rinker [33], which allows for second-(Uehling [34]) and fourth-order effects, including nuclear-size corrections,

$$V_U(r) = -\frac{Z\alpha^2}{3\pi}\int_{[1,\infty)} dt\left(\frac{2}{t^2}+\frac{1}{t^4}\right)(t^2-1)^{1/2} \times \int_{R^3} d^3r' \frac{\rho(\vec{r}\,')}{|\vec{r}-\vec{r}\,'|}e^{-2|\vec{r}-\vec{r}\,'|t}. \tag{6}$$

The fourth-order Wichmann-Kroll correction, is also included for higher accuracy [35]. These radiative terms are most important for inner-shell s electrons, which have the greatest density near the nucleus [36]. Figure 2 shows the extent, to which relativistic and QED interactions become important for the inner-shell ionization potentials as the nuclear charge Z increases.

III. COMPARISON WITH EXPERIMENTAL RESULTS

In order to assess the accuracy of the various approximations used [in particular, the Z expansion used in Eq. (5)], we calculated the K-$(1s)$ and L-$(2s)$ electron ionization potentials for the neutral atoms from hydrogen through to lawrencium, where experimental data are available [37], mostly from solid-state measurements. From Fig. 3, we see that the agreement between calculated and experimental values is excellent. Figure 4 shows more clearly the deviation of calculated values from experimental data. Agreement was obtained to a mean value of 7.2 eV for the K-shell and 12.8 eV for the L-shell, as summarized in Table I. This accuracy is more than sufficient if we consider that the current accuracy for measuring the kinetic energy of a K- or L-shell s electron is not less than 1 keV. In addition, Table I shows that the agreement is even better for the noble gases at 1.0 eV for the K shell, pointing toward the contribution of solid-state effects on the experimental data. Figure 4 clearly indicates that the accuracy is more or less independent in magnitude of the nuclear charge Z, and so becomes relatively less important as Z increases. Nevertheless, in the following, we shortly mention the sources of the remaining small errors.

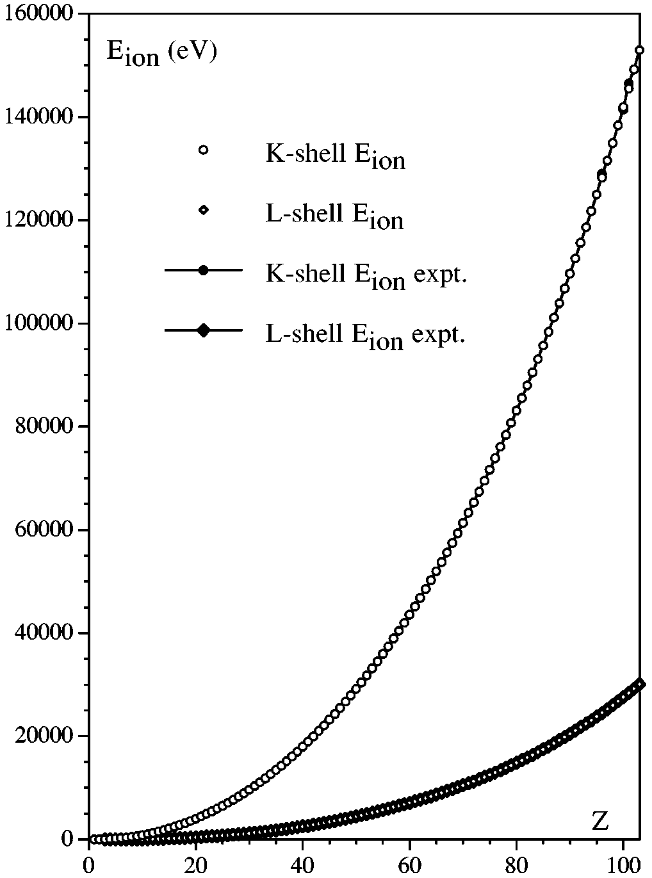

FIG. 3. Comparison between calculated and experimental $K(1s)$- and $L(2s)$- shell ionization potentials.

First, electron correlation effects and higher-order QED effects have been estimated to be of the order of 1 eV or less and may, therefore, be ignored [38] (see Ref. [39] for a detailed discussion). Second, the Z expansion used in Eq. (5) is not accurate for high Z. However, the small deviations from experiment up to Lr indicates that this error is at most a few eV's (this should be compared to the K-shell self-energy contribution for the ionization potential of Lr, which is 552 eV). Third, most of the experimental data come from solid state

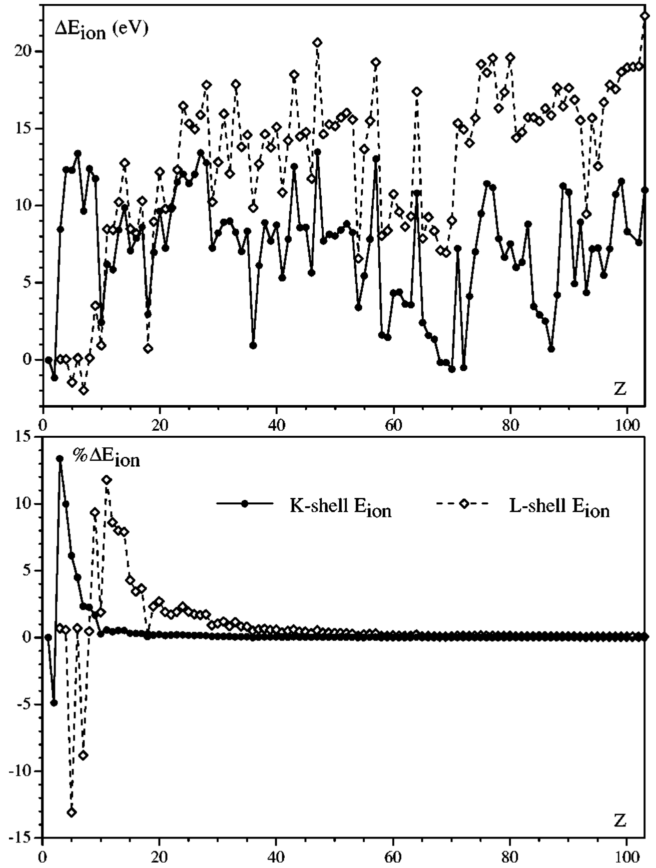

FIG. 4. Deviation of calculated from experimental $K(1s)$- and $L(2s)$-shell ionization potentials. $\Delta E_{ion}=E_{ion}(\text{calculated})-E_{ion}(\text{experimental})$. Experimental values from Ref. [37].

measurements and differences with the gas phase may well account for most of the deviation observed. In almost all cases, the experimental ionization potentials are less than the predicted values, notable exceptions being the early noble gases, where measurements come from the gas phase. In order to estimate such effects, we carried out solid-state calculations for Be, Mg, and Ca [40]. As expected, the $1s$ and $2s$ bandwidths are very small and not larger than 0.5 eV. However, compared to the isolated atom, the center of $1s$ band shifts upwards in energy by 3.2 eV for Be, 5.6 for Mg, and 5.0 for Ca. Similar results are obtained for the *L*-shell. This shift comes from the additional screening of the nucleus by the electrons at the neighboring atoms, which probably does not change significantly with increasing *Z* explaining the rather systematic deviations up to high *Z*. We mention, however, that the results obtained for the solid state are very sensitive to basis set effects and further investigations are necessary in order to obtain more accurate results. For Be we can also compare to experimental ionization potentials for the free atom, 123.6±0.1 eV for the *K* shell [41] and 9.320 eV for the *L* shell [42]. This compares to 123.3 and 8.045 eV respectively, the remaining difference due to electron correlation. For the *L* shell, Rn does not exhibit the same agreement as the other noble gases (which explains the larger standard deviation for the noble gas *L*-shell series shown in Table I), and effects other than the solid state are clearly more important for the heavier elements. Fourth, we mention that hyperfine effects (spin dependent and independent contributions) also contribute to some extent. For example, the superheavy nucleus can be highly deformed when *K* inversion takes place and nuclear-size effects can be quite large. For example, for $^{235}\text{U}^{90+}$ $(I=7/2)$, the change in the *K*-ionization potential is 186 eV at the DHF level of theory when going from a point nucleus to the two-parameter Fermi-charge distribution [36]. In contrast, mass correction and recoil terms are usually below 1 eV.

TABLE I. Agreement of calculated *K*- and *L*-shell ionization potentials with experimental data.

	Difference (eV)	*K* shell	*L* shell
H-Lr	Mean	7.20	12.77
	Standard deviation	3.69	5.34
	Maximum error	13.48	22.29
Noble Gases	Mean	1.02	6.88
	Standard deviation	2.39	6.53
	Maximum error	3.40	16.30

Shape deformation of the nucleus has been considered before by Blundell *et al.* [43], but only for ^{238}U which has $I=0$ and, therefore, a spherical average has been taken. In order to estimate nuclear deformation effects, we applied a nuclear quadrupole point-charge model as developed recently in our group for calculating electric-field gradients [44]. A quadrupole moment of 5 barns was used with $q=+4$ point charges placed at 7.9 fermi from the center of the nucleus (the estimated mean-square radius of element 118), and $q=-2$ point charges placed also at 7.9 fermi along the other two axes around the nucleus of charge $Z=118$ in order to preserve charge conservation. The model was applied self-consistently within the Dirac-Fock scheme using a rather large basis set of (*spd*) spinors close to the numerical Dirac-Fock limit. As expected, the influence of *p* spinors due to symmetry breaking by the deformed nucleus was found to be negligible. However, because of the quadrupolar symmetry *d* spinors should be included. According to our calculations, the quadrupole deformation increases the *K*-ionization potential by 10.9 eV (0.005% of the total ionization potential) for element 118 compared to the spherical charge distribution (for larger deformations, i.e., 7 barns, we obtain an increase of 9.3 eV). To put this result in perspective, we have a 3.34 keV decrease when going from a point nucleus to the two-parameter spherical Fermi charge distribution—in agreement with an earlier analysis by Carlson *et al.* [45]. Mohr *et al.* showed that using different models for the spherical charge distribution leads only to small deviations of about 1 eV for uranium [36]. Here, we confirm this result for element 118.

Considering the above, for element 118, we expect that the total error in the calculated ionization potential shown in Table II is of the order of a few 10 eV and, therefore, still below the experimental limit for *K*-conversion electrons which is about 1 keV. We mention that for $^{235}\text{U}^{90+}$, a quadrupole moment of $Q=4.9$ barns [46] leads to an increase of 1.7 eV in the ionization potential (0.0015% of the total ionization potential) from the spherical charge distribution.

TABLE II. *K*- and *L*-shell ionization potentials of the superheavy elements (in keV) dependent on the number of electrons (N_E) from $N_E = 1$ to $N_E = \mathrm{Z}$.

	K-shell E_{ion}				*L*-shell E_{ion}			
N_E	112	114	116	118	112	114	116	118
1	214.3125	224.6654	235.5554	246.9743				
2	210.9199	221.1209	231.8483	243.0944				
3	209.8640	220.0179	230.6946	241.8866	54.9549	57.8122	60.8359	64.0292
4	209.0459	219.1685	229.8119	240.9683	54.2934	57.1245	60.1202	63.2837
5	207.7215	217.7728	228.3385	239.4098	53.6036	56.4081	59.3753	62.5085
6	206.5557	216.5513	227.0563	238.0618	52.9784	55.7545	58.6909	61.7907
7	205.7465	215.7235	226.2097	237.1962	52.3749	55.1335	58.0520	61.1332
8	204.9679	214.9271	225.3955	236.3639	51.8168	54.5595	57.4615	60.5258
9	204.2203	214.1626	224.6139	235.5650	51.3041	54.0323	56.9194	59.9684
10	203.5020	213.4283	223.8633	234.7979	50.8359	53.5511	56.4248	59.4599
11	203.0824	212.9914	223.4082	234.3239	50.5105	53.2141	56.0758	59.0983
12	202.7238	212.6211	223.0254	233.9277	50.2273	52.9220	55.7741	58.7866
13	202.2496	212.1255	222.5070	233.3849	49.8822	52.5639	55.4022	58.4001
14	201.8106	211.6684	222.0304	232.8875	49.5427	52.2120	55.0372	58.0212
15	201.4680	211.3174	221.6709	232.5194	49.2518	51.9136	54.7311	57.7072
16	201.1349	210.9761	221.3214	232.1615	48.9664	51.6209	54.4310	57.3995
17	200.8112	210.6446	220.9819	231.8139	48.6866	51.3340	54.1370	57.0982
18	200.4967	210.3225	220.6522	231.4764	48.4120	51.0528	53.8489	56.8032
19	200.1685	209.9862	220.3078	231.1238	48.1007	50.7339	53.5215	56.4672
20	199.8460	209.6559	219.9695	230.7775	47.7922	50.4174	53.1969	56.1344
21	199.5295	209.3317	219.6375	230.4377	47.4864	50.1037	52.8752	55.8047
22	199.2186	209.0132	219.3114	230.1038	47.1834	49.7925	52.5563	55.4779
23	198.9250	208.7132	219.0050	229.7910	46.8920	49.4944	52.2516	55.1665
24	198.6349	208.4167	218.7020	229.4816	46.6061	49.2019	51.9524	54.8606
25	198.3482	208.1237	218.4027	229.1758	46.3257	48.9149	51.6589	54.5604
26	198.0653	207.8344	218.1071	228.8739	46.0509	48.6337	51.3711	54.2660
27	197.7857	207.5486	217.8151	228.5757	45.7814	48.3578	51.0887	53.9772
28	197.5094	207.2662	217.5264	228.2808	45.5170	48.0870	50.8115	53.6936
29	197.3165	207.0661	217.3171	228.0647	45.3524	47.9168	50.6352	53.5110
30	197.1435	206.8872	217.1336	227.8736	45.2006	47.7601	50.4738	53.3445
31	196.9368	206.6718	216.9091	227.6394	45.0316	47.5851	50.2924	53.1565
32	196.7413	206.4685	216.6977	227.4193	44.8649	47.4125	50.1136	52.9712
33	196.5792	206.3021	216.5268	227.2441	44.7184	47.2620	49.9591	52.8127
34	196.4206	206.1392	216.3597	227.0726	44.5739	47.1137	49.8068	52.6563
35	196.2656	205.9800	216.1963	226.9050	44.4315	46.9674	49.6567	52.5022
36	196.1139	205.8244	216.0366	226.7411	44.2910	46.8232	49.5087	52.3504
37	195.9608	205.6670	215.8750	226.5752	44.1424	46.6706	49.3519	52.1893
38	195.8099	205.5120	215.7157	226.4119	43.9951	46.5192	49.1964	52.0296
39	195.6613	205.3593	215.5589	226.2509	43.8492	46.3692	49.0423	51.8713
40	195.5149	205.2088	215.4044	226.0922	43.7047	46.2205	48.8893	51.7142
41	195.3749	205.0653	215.2572	225.9414	43.5649	46.0769	48.7421	51.5632
42	195.2365	204.9233	215.1116	225.7921	43.4271	45.9355	48.5970	51.4144
43	195.0997	204.7828	214.9676	225.6446	43.2916	45.7964	48.4542	51.2680
44	194.9644	204.6440	214.8252	225.4985	43.1582	45.6594	48.3136	51.1237
45	194.8307	204.5067	214.6844	225.3541	43.0269	45.5246	48.1752	50.9817
46	194.6984	204.3709	214.5450	225.2113	42.8977	45.3918	48.0389	50.8419
47	194.5715	204.2405	214.4110	225.0737	42.7682	45.2587	47.9022	50.7016
48	194.4461	204.1115	214.2785	224.9375	42.6404	45.1273	47.7671	50.5628
49	194.3224	203.9842	214.1476	224.8031	42.5142	44.9975	47.6338	50.4259
50	194.2004	203.8587	214.0185	224.6705	42.3898	44.8696	47.5023	50.2908
51	194.0799	203.7347	213.8910	224.5394	42.2671	44.7433	47.3724	50.1574

TABLE II. (*Continued.*)

	K-shell E_{ion}				L-shell E_{ion}			
N_E	112	114	116	118	112	114	116	118
52	193.9610	203.6123	213.7651	224.4101	42.1459	44.6186	47.2442	50.0258
53	193.8452	203.4930	213.6424	224.2840	42.0277	44.4970	47.1192	49.8974
54	193.7307	203.3752	213.5212	224.1593	41.9111	44.3769	46.9957	49.7704
55	193.6120	203.2588	213.4014	224.0362	41.7902	44.2584	46.8738	49.6451
56	193.5062	203.1439	213.2832	223.9146	41.6824	44.1414	46.7535	49.5214
57	193.3874	203.0306	213.1665	223.7945	41.5617	44.0262	46.6348	49.3993
58	193.2861	202.9188	213.0513	223.6760	41.4585	43.9125	46.5178	49.2789
59	193.1809	202.8085	212.9376	223.5590	41.3515	43.8003	46.4022	49.1600
60	193.0753	202.6995	212.8253	223.4433	41.2442	43.6897	46.2882	49.0426
61	192.9890	202.6099	212.7318	223.3458	41.1662	43.6086	46.2040	48.9548
62	192.9096	202.5270	212.6457	223.2564	41.0923	43.5319	46.1244	48.8726
63	192.8218	202.4351	212.5494	223.1555	41.0149	43.4513	46.0403	48.7851
64	192.7376	202.3471	212.4574	223.0593	40.9385	43.3717	45.9575	48.6988
65	192.6656	202.2725	212.3803	222.9797	40.8705	43.3014	45.8848	48.6237
66	192.5950	202.1994	212.3046	222.9015	40.8035	43.2320	45.8130	48.5496
67	192.5258	202.1277	212.2305	222.8247	40.7374	43.1636	45.7423	48.4764
68	192.4579	202.0574	212.1577	222.7496	40.6723	43.0961	45.6725	48.4043
69	192.3924	201.9893	212.0872	222.6765	40.6075	43.0289	45.6028	48.3321
70	192.3278	201.9223	212.0176	222.6045	40.5435	42.9624	45.5339	48.2607
71	192.2643	201.8563	211.9492	222.5335	40.4803	42.8968	45.4658	48.1901
72	192.2018	201.7914	211.8818	222.4637	40.4179	42.8319	45.3984	48.1203
73	192.1419	201.7292	211.8173	222.3968	40.3576	42.7693	45.3335	48.0530
74	192.0828	201.6678	211.7537	222.3310	40.2984	42.7078	45.2697	47.9869
75	192.0245	201.5998	211.6909	222.2658	40.2401	42.6397	45.2068	47.9217
76	191.9672	201.5476	211.6289	222.2016	40.1828	42.5877	45.1450	47.8576
77	191.9106	201.4888	211.5678	222.1383	40.1266	42.5292	45.0842	47.7946
78	191.8548	201.4308	211.5076	222.0757	40.0712	42.4716	45.0244	47.7324
79	191.8044	201.3780	211.4525	222.0184	40.0199	42.4179	44.9684	47.6742
80	191.7547	201.3260	211.3982	221.9619	39.9694	42.3651	44.9132	47.6167
81	191.7060	201.2750	211.3449	221.9061	39.9199	42.3132	44.8590	47.5601
82	191.6582	201.2249	211.2925	221.8514	39.8714	42.2624	44.8058	47.5046
83	191.6113	201.1757	211.2409	221.7977	39.8238	42.2124	44.7535	47.4500
84	191.5653	201.1273	211.1903	221.7447	39.7771	42.1633	44.7021	47.3963
85	191.5207	201.0805	211.1411	221.6933	39.7318	42.1157	44.6522	47.3441
86	191.4770	201.0344	211.0928	221.6426	39.6874	42.0690	44.6032	47.2927
87	191.4322	200.9892	211.0453	221.5929	39.6421	42.0232	44.5550	47.2423
88	191.3921	200.9449	210.9987	221.5441	39.6014	41.9783	44.5078	47.1928
89	191.3481	200.9016	210.9531	221.4962	39.5569	41.9344	44.4616	47.1443
90	191.3104	200.8592	210.9083	221.4491	39.5187	41.8915	44.4163	47.0966
91	191.2718	200.8176	210.8645	221.4029	39.4796	41.8494	44.3719	47.0498
92	191.2334	200.7769	210.8214	221.3575	39.4409	41.8083	44.3284	47.0040
93	191.1989	200.7400	210.7804	221.3162	39.4083	41.7736	44.2917	46.9650
94	191.1663	200.7055	210.7456	221.2772	39.3770	41.7405	44.2565	46.9281
95	191.1332	200.6699	210.7075	221.2366	39.3462	41.7075	44.2214	46.8909
96	191.1013	200.6356	210.6709	221.1975	39.3160	41.6752	44.1870	46.8542
97	191.0741	200.6065	210.6400	221.1649	39.2894	41.6469	44.1569	46.8225
98	191.0475	200.5781	210.6098	221.1329	39.2635	41.6191	44.1275	46.7913
99	191.0217	200.5505	210.5803	221.1016	39.2381	41.5920	44.0986	46.7607
100	190.9965	200.5236	210.5516	221.0710	39.2134	41.5655	44.0704	46.7307
101	190.9744	200.4995	210.5257	221.0434	39.1913	41.5415	44.0445	46.7031
102	190.9530	200.4762	210.5005	221.0164	39.1699	41.5182	44.0193	46.6760
103	190.9324	200.4536	210.4760	220.9900	39.1492	41.4955	43.9947	46.6496

TABLE II. (*Continued.*)

	K-shell E_{ion}				L-shell E_{ion}			
N_E	112	114	116	118	112	114	116	118
104	190.9125	200.4317	210.4522	220.9643	39.1292	41.4735	43.9708	46.6238
105	190.8939	200.4112	210.4298	220.9401	39.1105	41.4528	43.9482	46.5993
106	190.8761	200.3913	210.4080	220.9164	39.0926	41.4328	43.9263	46.5755
107	190.8591	200.3722	210.3869	220.8934	39.0755	41.4137	43.9051	46.5524
108	190.8431	200.3540	210.3666	220.8713	39.0594	41.3953	43.8847	46.5302
109	190.8279	200.3365	210.3470	220.8497	39.0442	41.3778	43.8651	46.5086
110	190.8138	200.3198	210.3282	220.8289	39.0300	41.3611	43.8462	46.4877
111	190.8028	200.3064	210.3128	220.8116	39.0192	41.3481	43.8313	46.4710
112	190.7928	200.2942	210.2985	220.7954	39.0094	41.3359	43.8172	46.4551
113		200.2834	210.2853	220.7801		41.3254	43.8044	46.4403
114		200.2737	210.2731	220.7656		41.3159	43.7924	46.4261
115			210.2638	220.7543			43.7831	46.4149
116			210.2555	220.7435			43.7748	46.4041
117				220.7337				46.3943
118				220.7248				46.3855

Since current accuracy in level calculations for uranium atoms is aimed towards 0.1 eV or better, this effect deserves some further investigations. However, our point-charge model is fairly crude and to estimate nuclear deformation effects to high accuracy the proton charge distribution has to be modeled better (e.g., it should be taken from microscopic nuclear calculations). This will be the subject of our future investigations.

We finally mention a rather large discrepancy between the calculated and recommended K-ionization potentials for Md ($Z=101$) [47] of almost 1 keV. Since our values are fully within the expected trend (Fig. 3), we suspect the experimental value of 146.780 keV to be wrong (theoretical value is 145.537 keV). Moreover, our value is in rather good agreement with the one published by Carlson *et al.* [45] obtained from Hartree-Fock-Slater K-shell orbital energies (145.571 keV).

IV. IONIZATION POTENTIALS

Potentials were calculated for all states of ionization, that is, the number of electrons was varied between $N_E=1$ and $N_E=Z$ with all atoms kept in the electronic ground state. For future experimental and theoretical use, all data are listed in Table II. The results are also presented in Fig. 5, which clearly illustrates the effects of outer electrons shielding the nucleus (change from Z to an effective nuclear charge with $Z_{eff}<Z$) and lowering the ionization potential for the inner electrons with increasing N_E. In fact, we see an exponential decrease in the ionization potential with increasing N_E, that is, the largest screening comes from the inner-shell electrons as one might expect. The ionization potential can thus be approximated in a series of exponentials,

$$\Delta E_{K,L}=E_H(Z)+\sum_i f_i(Z)e^{-\alpha_i(N_E-1)}. \tag{7}$$

$E_H(Z)$ is the ionization potential of the hydrogenlike atom with nuclear charge Z, i.e., we have $N_E=1$. The values for $E_H(Z)$ are in the first row of Table II. The coefficients $f_i(Z)$ are also Z dependent and can be fitted to high accuracy with a linear function,

$$f_i(Z)=a_i+b_iZ. \tag{8}$$

The coefficients are listed in Table III for a sum of four exponentials, which is reasonably accurate. This formula should also give a useful approximation for odd nuclear charges in the region $Z=111$–119.

Figure 6 shows the effect of the Breit interaction on the ionization potential of the $1s$ and $2s$ electrons. For the K shell, this is the most important contribution, at 0.55% of the ionization potential for the neutral element 118, but it is only 0.39% of the L shell ionization potential for element 118. The self-energy term (see Figs. 1 and 2) becomes more important for the L shell in the superheavy region, at 0.47% of the ionization potential for 118. The vacuum polarization is the smallest of these corrections for both the K- and L-shell ionization potential (Fig. 2). Table IV summarizes the percentage contribution of the Breit, self-energy and vacuum polarization interactions to the K- and L-shell ionization potential of the neutral elements 112, 114, 116, and 118.

As expected, the total Breit contribution increases in magnitude as electrons are added. However, there is a competing effect of screening by the outer electrons that reduces the magnetic energy contributions of the inner electrons [48]. This results in the maximum contribution occurring at the 35th ($4p^3$) electron for the K shell and at the 25th ($3d^3$) electron for the L shell. The short-range nature of the Breit interaction is illustrated by the dominance of the contribution of the $1s$ electrons. For elements 112–118, they are responsible for 67% of the total Breit contribution to the K-shell ionization potential in the neutral element. For the L shell, the Breit interaction of the two $2s$ electrons composes only

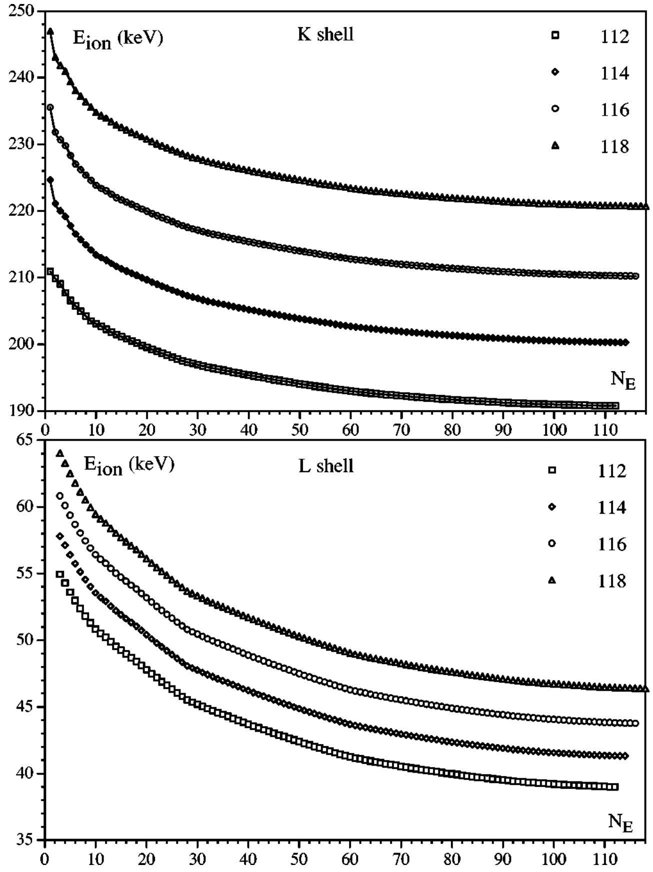

FIG. 5. Calculated $K(1s)$- and $L(2s)$-shell ionization potentials (see Table II for actual numbers) for the elements with $Z=112$, 114, 116, and 118 dependent on the number of electrons N_E.

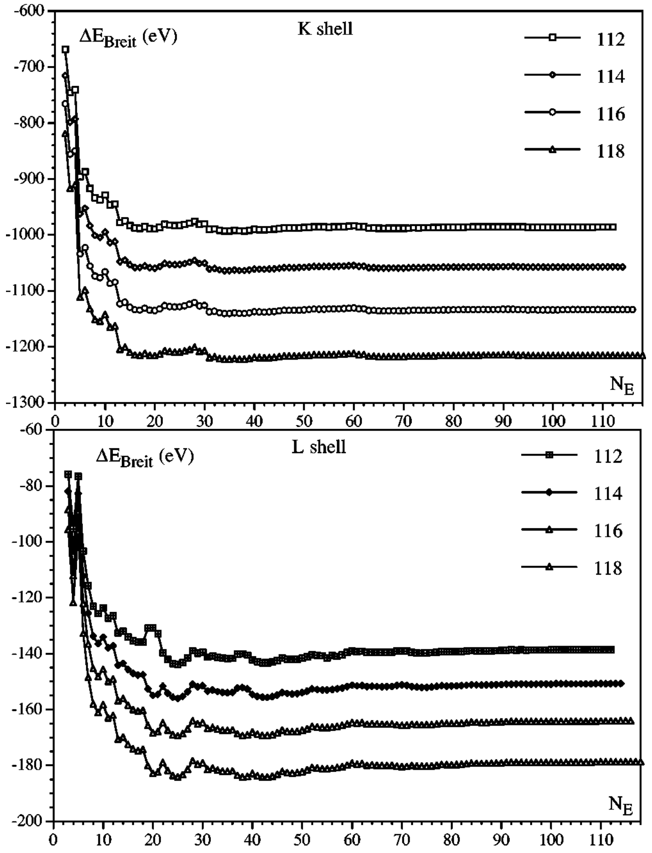

FIG. 6. Total Breit contributions for the elements with $Z=112$, 114, 116, and 118 dependent on the number of electrons N_E.

54% of the total Breit contribution. The retardation part of the Breit term that requires the inclusion of frequency dependence for the exchange photon adjusts the total contribution of the Breit term to the *K*-shell ionization potential by around 3% for the neutral elements. Figure 6 also shows shell effects, which are not so easily seen for the total ionization potentials (Fig. 5). For example, introducing an electron to an already closed-shell system leads to only a small addition in the Breit contribution reflected by the peaks presented in Fig. 6. Such shell effects are more pronounced in the inner-shell region, where the total Breit interaction shows larger variations.

TABLE III. Parameters for the coefficients given in Eqs. (7) and (8) (in keV). The values for the H-like ionization potentials $E_H(Z)$ are given in the first row of Table II. The standard and maximum deviations are also given.

	K	L
a_1	-13.8069	-7.69403
a_2	-5.29836	4.26191
a_3	19.9408	-30.0979
a_4	1.03811	31.3147
b_1	0.189908	0.096034
b_2	0.194717	0.121685
b_3	-0.398961	0.261948
b_4	-0.007960	0.445383
α_1	0.223993	0.169218
α_2	0.026636	0.023054
α_3	0.000171	0.006286
α_4	0.015783	0.000807
Standard deviation	0.051	0.052
Maximum deviation	0.129	0.174

Both the self-energy and vacuum polarization contributions decrease in magnitude with increasing number of electrons N_E, and reach a plateau after filling the first two or three shells (Fig. 7). This can easily be understood since adding electrons leads to a more effective screening of the nucleus and diminishes the major QED contributions coming from the $1s$ and $2s$ shells., i.e., for the K shell, the outer

TABLE IV. Contributions to the ionization potential of the neutral atom.

% of E_{ion}		112	114	116	118
K	Breit	-0.52	-0.53	-0.54	-0.55
	SE	-0.43	-0.45	-0.47	-0.50
	VP	0.16	0.17	0.19	0.20
L	Breit	-0.36	-0.36	-0.37	-0.39
	SE	-0.40	-0.42	-0.44	-0.47
	VP	0.15	0.17	0.18	0.20

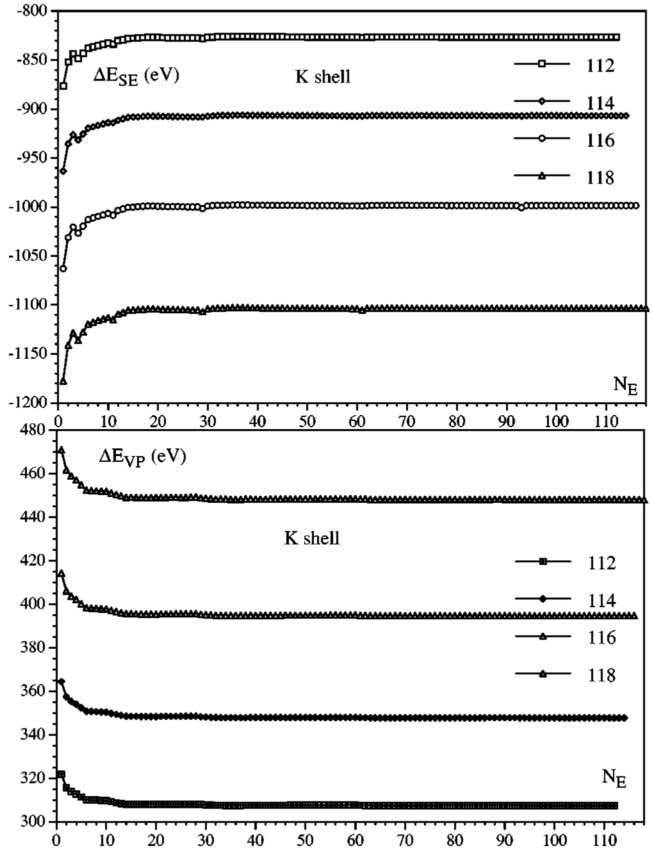

FIG. 7. Self-energy (SE) and vacuum polarization contributions for the elements with $Z=112$, 114, 116, and 118 dependent on the number of electrons N_E.

electrons reduce the 1s-electron self-energy by 6–6.5 %. For the *L* shell, the effect is even larger, 13–14 %, again since the 2*s* electron is more exposed to the shielding effects of the outer electrons. We mention that the self-energy contributions diminish to 0.50% of the total ionization potential for the *K* shell of element 118, and to 0.47% for the *L*-shell ionization potential. The vacuum polarization contribution to the ionization potential has the opposite sign to the Breit and SE terms, and is 0.2% of the total ionization potential for both the *K* and the *L* shells in 118. The outer electrons reduce the *K* electron VP by 5%, and 9% for the *L* shell.

Finally, we mention early Hartree-Fock-Slater calculation by Carlson *et al.* [45]. Their *K*- and *L*-shell energies have been obtained from Koopmans' theorem for the neutral elements from $Z=96$–120. A comparison with our values for 112, 114, 116, and 118 shows agreement within 0.4 keV.

V. CONCLUSIONS

The calculations presented in this paper have been undertaken in order to provide useful data for use in conversion electron spectroscopy of the heaviest and superheavy elements. The hope is that future experiments may well be able to use electron conversion for the nuclear charge identification of superheavy elements. From nuclear structure calculations and systematics of experimental data, one may be able to estimate nuclear rotational levels to an accuracy of a few keV. Thus, the accuracy of the order of several 10 eV for the ionization potentials obtained in this work, by including relativistic and quantum electrodynamical corrections, is more than sufficient for potential use in an experiment aiming at element identification. The major effects not taken into account are electron correlation and higher-order QED, which are expected to be of the order of 1 eV or less. However, we mention that nuclear deformation effects, i.e., the deviation from a spherical nuclear charge distribution may become even more important than these higher-order QED terms. We leave this subject to future investigations employing charge distributions obtained in self-consistent nuclear structure calculations.

As a by-product of our work, we performed systematic calculations of $K-(1s)$ and $L-(2s)$ ionization potentials for the neutral atoms from hydrogen to lawrencium and obtained excellent agreement with experiment. The major cause of the almost systematic 5–10 eV deviation from experiment seems to come from solid-state effects present in the experimental data.

The most stable superheavy elements are expected to be spherical. However, their α-decay products may be deformed and subject to detection by *K*-conversion spectroscopy. Finally, let us mention that by taking the difference between *K*- and *L*-ionization potentials calculated in this work, one obtains the energy of the x-ray transition characteristic of a specific element. Unfortunately, the probability of a shake-off of the 1*s* orbit in a heavy element is prohibitively small [20].

ACKNOWLEDGMENTS

We would like to thank J. Sapirstein (Notre Dame), D. Andrae (Bielefeld), and Sigurd Hoffman (GSI Darmstadt) for valuable discussions. This work was supported by the Marsden Fund managed by the Royal Society of New Zealand and the Auckland University Research Committee, and by the US Department of Energy under Contract Nos. DE-FG02-96ER40963 (University of Tennessee), and DE-AC05-00OR22725 with UT-Battelle, LLC (Oak Ridge National Laboratory).

---

[1] P.H. Heenen and W. Nazarewicz, Europhys. News **33**, 5 (2002); S. Hofmann and G. Münzenberg, Rev. Mod. Phys. **72**, 733 (2000).
[2] G. Münzenberg, Nucl. Phys. A **693**, 207 (2001).
[3] Yu.Ts. Oganessian, A.V. Yeremin, A.G. Popeko, O.N. Malyshev, and A.B. Yakushev, J. Nucl. Radiochem. Sci. **3**, 217 (2002).
[4] S. Hofmann *et al.*, Eur. Phys. J. A **14**, 147 (2002).
[5] Yu.Ts. Oganessian, J. Nucl. Radiochem. Sci. **3**, 5 (2002).
[6] Yu.Ts. Oganessian *et al.*, Nature (London) **400**, 242 (1999); Phys. Rev. C **62**, 041604 (2000); **63**, 011301 (2001).
[7] Yu.Ts. Oganessian, A.V. Yeremin, A.G. Popeko, O.N. Malyshev, and A.B. Yakushev, J. Nucl. Radiochem. Sci. **3**, 217 (2002).

[8] T.C. Tucker, L.D. Roberts, C.W. Nestor, Jr., T.A. Carlson, and F.B. Malik, Phys. Rev. **174**, 118 (1968).
[9] D. Gassmann *et al.*, Phys. Lett. B **497**, 181 (2001).
[10] P. Reiter *et al.*, Phys. Rev. Lett. **82**, 509 (1999); R.-D. Herzberg *et al.*, Phys. Rev. C **65**, 014303 (2001); P. Reiter *et al.*, in *Nuclear Structure and Formation Mechanism of Heavy Shell-stabilized Nuclei*, edited by E. Norman, L. Schroeder, and G. Wozniak, AIP Conf. Proc. No. 610 (AIP, Melville, NY, 2002), p. 756.
[11] P.A. Butler *et al.*, Nucl. Instrum. Methods Phys. Res. A **381**, 433 (1996).
[12] W. Nazarewicz and I. Ragnarsson, in *Handbook of Nuclear Properties*, edited by D. Poenaru and W. Greiner (Oxford Science Publications/Clarendon Press, Oxford, 1996), p. 80.
[13] T. Duguet, P. Bonche, and P.-H. Heenen, Nucl. Phys. A **679**, 427 (2001); A. Sobiczewski, I. Muntian, and Z. Patyk, Phys. Rev. C **63**, 034306 (2001); J.L. Egido and L.M. Robledo, Phys. Rev. Lett. **85**, 1198 (2000).
[14] F.P. Hessberger *et al.*, Eur. Phys. J. A **12**, 57 (2001); F.P. Hessberger, S. Hofmann, D. Ackermann, A.G. Popeko, S. Saro, and A.V. Yeremin, Institute Report No. GSI 2002-1, 2002 (unpublished).
[15] S. Cwiok, J. Dobaczewski, P.-H. Heenen, P. Magierski, and W. Nazarewicz, Nucl. Phys. A **611**, 211 (1996); A. Sobiczewski, Z. Patyk, and S. Cwiok, Phys. Lett. B **224**, 1 (1989); P. Möller and J.R. Nix, J. Phys. G **20**, 1681 (1994).
[16] S. Cwiok, W. Nazarewicz, and P.-H. Heenen, Phys. Rev. Lett. **83**, 1108 (1999).
[17] G. Münzenberg, Nucl. Phys. A **690**, 175 (2001).
[18] O. Dragoun, M. Rysavy, and A. Spalek, J. Phys. G **26**, 1461 (2000); M. Rysavy and O. Dragoun, At. Data Nucl. Data Tables **78**, 129 (2001).
[19] P. Schlüter, U. Müller, G. Soff, Th. de Reus, J. Reinhardt, and W. Greiner, Z. Phys. A **323**, 139 (1986).
[20] J.S. Levinger, Phys. Rev. **90**, 11 (1953); J.P. Briand, P. Chevallier, A. Johnson, J.P. Rozet, M. Tavernier, and A. Touati, Phys. Rev. Lett. **33**, 266 (1974); J.S. Hansen, Phys. Rev. A **9**, 40 (1974); M.S. Rapaport, F. Asaro, and L. Perlman, Phys. Rev. C **11**, 1740 (1975); R. Anholt and P.A. Amundsen, Phys. Rev. A **25**, 169 (1982).
[21] P. Pyykkö, Chem. Rev. **88**, 563 (1988).
[22] P. Pyykkö, M. Tokman, and L.N. Labzowsky, Phys. Rev. A **57**, R689 (1998); L.N. Labzowsky, I. Goidenko, M. Tokman, and P. Pyykkö, *ibid.* **59**, 2701 (1999).
[23] K.G. Dyall, I.P. Grant, C.T. Johnson, F.A. Parpia, and E.P. Plummer, Comput. Phys. Commun. **55**, 425 (1989).
[24] D. Andrae, Phys. Rep. **336**, 413 (2000).
[25] C.C. Lu, T.A. Carlson, F.B. Malik, T.C. Tucker, and C.W. Nestor, At. Data **3**, 1 (1968).
[26] M. Reiher and C. Kind, J. Phys. B **34**, 3133 (2001).
[27] M.H. Mittleman, Phys. Rev. A **4**, 893 (1971); **5**, 2395 (1972).
[28] L. Gaunt, Proc. R. Soc. London, Ser. A **122**, 513 (1929); G. Breit, Phys. Rev. **34**, 553 (1929); **39**, 616 (1932).
[29] P.J. Mohr, Ann. Phys. (N.Y.) **88**, 26 (1974).
[30] P.J. Mohr, Phys. Rev. A **46**, 4421 (1992); P.J. Mohr and Y.K. Kim, *ibid.* **45**, 2727 (1992).
[31] K.T. Cheng, W.R. Johnson, and J. Sapirstein, Phys. Rev. A **47**, 1817 (1993).
[32] J. Sapirstein, Rev. Mod. Phys. **70**, 55 (1998).
[33] L.W. Fullerton and G.A. Rinker, Jr., Phys. Rev. A **13**, 3 (1976).
[34] E.A. Uehling, Phys. Rev. **48**, 55 (1935).
[35] E.H. Wichmann and N.M. Kroll, Phys. Rev. **96**, 232 (1954); **96**, 843 (1956).
[36] P.J. Mohr, G. Plunien, and G. Soff, Phys. Rep. **293**, 227 (1998). Table II on p. 265 gives values in keV.
[37] F.B. Larkins, At. Data Nucl. Data Tables **20**, 313 (1977); K. D. Sevier, *Low Energy Electron Spectroscopy* (Wiley-Interscience, New York, 1972); F.T. Porter and M.S. Freedman, J. Phys. Chem. Ref. Data **7**, 1267 (1978).
[38] Ch. Briançon and J.P. Desclaux, Phys. Rev. A **13**, 6 (1976).
[39] I. Lindgren, Int. J. Quantum Chem. **57**, 683 (1996).
[40] V.R. Saunders, R. Dovesi, C. Roetti, M. Causà, N.H. Harrison, R. Orlando, and C.M. Zicovich-Wilson, Computer code CRYSTAL98 (University of Torino, Torino, 1998).
[41] P. Bisgaard, R. Bruch, P. Dahl, B. Fastrup, and M. Rødbro, Phys. Scr. **17**, 49 (1978).
[42] C.E. Moore, *Atomic Energy Levels*, Natl. Bur. Stand. (U.S.) Circ. No. 467 (U.S. GPO, Washington, D.C., 1958).
[43] S.A. Blundell, W.R. Johnson, and J. Sapirstein, Phys. Rev. A **41**, 1698 (1990).
[44] M. Pernpointner, M. Seth, and P. Schwerdtfeger, J. Chem. Phys. **108**, 6722 (1998).
[45] T.A. Carlson, C.W. Nestor, Jr., F.B. Malik, and T.C. Tucker, Nucl. Phys. A **135**, 57 (1969).
[46] P. Pyykkö, Mol. Phys. **99**, 1617 (2001).
[47] J. Bearden and A.F. Burr, Rev. Mod. Phys. **39**, 125 (1967).
[48] P. Indelicato, J. Phys. B **19**, 1719 (1986).